Structural and Motional Features of a Layered Sodium Hydrous Silicate as Revealed by Solid State NMR

Carole Gardiennet and Piotr Tekely*

Laboratoire de Méthodologie RMN, FRE CNRS 2415, Université Henri Poincaré, Nancy 1, 54500 Vandoeuvre-lès-Nancy, France

Received: February 25, 2002; In Final Form: May 24, 2002

An approach for the investigation of layered alkali metal polysilicate hydrous materials is presented by choosing complementary multinuclear NMR methodologies. New insights into the structural and motional features of magadiite, a layered sodium silicate hydrate, have been gained using ^{1}H, ^{2}H, ^{29}Si and ^{23}Na one- and two-dimensional NMR experiments. Complementary ^{1}H MAS single- and double-quantum studies have proven to be powerful tools in a clear recognition of the nature of hydrous species involved in hydrogen bonding. ^{1}H and ^{2}H MAS experiments permitted us to determine the extent of the mobility of water molecules and provided corroborating evidences of an intralayer, strongly hydrogen bonded character of silanol groups. On the basis of a novel strategy in the analysis of the cross polarization dynamics, it appeared that magadiite contains two types of structurally different $Q^{(3)}$ tetrahedra, as well as two types of sodium ions. The strategy applied in this work might be useful to obtain structural and motional information in the related layered alkali metal silicates, as well as in other classes of nanoporous materials.

Introduction

Magadiite and kenyaite were the first described natural hydrous sodium silicates with sheet structure.[1] Nowadays, around 10 layered sodium silicates are known and can be easily synthesized.[2−6] However, in most cases, apart from makatite,[4] kanemite,[5] and RUB-18,[6] the crystal structure remains unknown because crystals of both natural and synthetic samples are of colloidal size and are only available in a finely divided form. Hydrated sodium silicates are active in the sorption of water and polar organic molecules,[2] and the interlayer sodium ions are easily ion- or proton-exchanged.[7] These properties permit us to use the sodium silicates in adsorbent, catalytic, and detergent systems[3]. Very recently, it has been also reported that magadiite can be used in the synthesis of composite mesoporous materials by the intercalation of silica between the magadiite layers.[8]

Magadiite, the most frequently researched, with the idealized formula $Na_2Si_{14}O_{29}{\cdot}nH_2O$ ($n = 8-10$), has a multilayer structure, the sodium ions and water molecules being placed between the layers.[1−5] Its basal spacing of ca. 15.4−15.8 Å decreases by ca. 3−4 Å upon dehydration.[2−3,9−10] Previous ^{29}Si MAS NMR studies showed the presence of $Q^{(3)}$ silicons (bound to three [SiO_4] tetrahedra and one OH group) and $Q^{(4)}$ silicons (bound only to [SiO_4]) in the basic layer structure of magadiite.[3,11,12] The ratio of $Q^{(3)}$:$Q^{(4)}$ close to 1:3 was determined by ^{29}Si MAS NMR single pulse experiments.[13,14] Strong hydrogen bonding of silanol protons has been reported by ^{1}H MAS NMR[12] and IR[15] studies, however the origin of involved oxygens has not been identified so far. ^{23}Na MAS NMR experiments on synthetic magadiite samples have revealed a unique sodium site in octahedral coordination with relatively high symmetry.[16,17]

Despite the above-mentioned studies, further investigations are necessary to clarify the structure of magadiite, a similar situation occurring for most of the related layered sodium silicates. In addition to the problem of connectivity of the $Q^{(3)}$ and $Q^{(4)}$ tetrahedra, the information on the nature of hydrogen bonding is strongly desired. In fact, the intercalation of polar molecules can be dramatically controlled by the existence of interlayer hydrogen bonds. The presence of hydrogen bonding involving OH groups and oxygens of the next layer has been proposed in the hypothetical model structure of these compounds by Almond and co-workers.[18] From the IR spectrum of magadiite, Huang et al.[15] also concluded that the OH groups are involved in interlayer hydrogen bonding. On the other hand, Eypert−Blaison et al.[19] deduced from IR study that at a higher hydration level, adsorbed water molecules in magadiite "are mainly in a strongly hydrogen bonded state". Such divergent conclusions clearly deserve further investigations to clarify the local bonding environment of the hydrogen species. There is also another important question of the dynamic and structural characteristics of the various interlayer species into which previous studies have offered little insight. Indeed, apart from the influence of the environment on molecular motion, the dynamics of water molecules and the emplacement of sodium ions in these catalytically active materials are of particular importance.

The main aims of our contribution to this field are to examine the extent and the nature of hydrogen bonding of hydrous species and to characterize the amount of molecular mobility of water molecules in magadiite. For this, we present here the detailed analysis of the ^{1}H−^{29}Si and ^{1}H−^{23}Na cross-polarization dynamics and high-resolution solid-state ^{1}H single- and double-quantum NMR experiments. Complementary 2D heteronuclear shift correlation experiments as well as ^{2}H MAS spectra are

* To whom correspondence should be addressed. E-mail: Piotr.Tekely@rmn.uhp-nancy.fr. Address: Laboratoire de Méthodologie RMN, Université Henri Poincaré, Nancy 1, 54500 Vandoeuvre-lès-Nancy, France. Fax: (33) 383684347. Tel: (33) 383684352.

10.1021/jp0256443 CCC: $22.00
Published on Web 08/08/2002

presented and analyzed in terms of geometrical and motional features of interlayer species.

Experimental Section

Materials. The synthetic Na-magadiite sample used in this work was prepared as described elsewhere.[19] For ^{2}H MAS studies, the sample was dried under vacuum over 24 h and rehydrated with pure D_2O.

NMR Methodologies. All measurements were carried out on a Bruker DSX300 spectrometer in a magnetic field of 7.0 T (proton frequency of 300.13 MHz), with MAS probe for a 4 mm rotor. Different one- and two-dimensional NMR experiments have been used in this work. Single pulse ^{1}H, ^{2}H and ^{23}Na and ^{29}Si MAS spectra have been recorded at different spinning frequencies. ^{1}H double quantum experiments were carried out by using the five-pulse, rotor synchronized sequence.[20,21] The standard[22] and modified[23] variable-contact cross polarization (CP) experiments were used. The ^{1}H−X (^{29}Si or ^{23}Na) correlation experiment has also employed the CP procedure.[24]

Preparing Appropriate Conditions for ^{1}H→^{29}Si Hartmann−Hahn Cross Polarization Under Fast Magic-Angle Spinning. Although the easiest way to record the quantitative ^{29}Si NMR spectrum is a direct excitation by a single pulse, this cannot be reasonably applied in most inorganic solids due to their extremely long ^{29}Si longitudinal relaxation times. Such a situation takes place also in our magadiite sample showing a continuous increase of the intensity of ^{29}Si MAS spectra recorded by a single pulse excitation with a repetition time up to 4000 s. In fact, previous silicon-29 T_1 relaxation time measurements[14] indicate the values ranging from 150 to 270 s for $Q^{(3)}$ and from 500 to 900 s for $Q^{(4)}$ of synthetic and natural magadiite, respectively. Such long relaxation times preclude any possibility of a systematic quantitative study involving direct observation of ^{29}Si nuclei. Although the feasibility of recording single pulse ^{29}Si MAS spectra of magadiite with the repetition time of 5 s has been reported,[19] this was most probably due to the presence of paramagnetic contamination which can accelerate the relaxation of a small part of sample and permits to record spectra with intensities being fortuitously similar to the fully relaxed quantitative spectra. To avoid such problems, we will take advantage of magnetization transfer from protons to ^{29}Si spins. Despite the fact that, when using CP procedure, the quantitative proportions of chemically or crystallographically inequivalent sites cannot be reached as with single pulse excitation, extremely valuable structural and dynamic information can be obtained in this manner. However, when recording the CP spectra under MAS at spinning frequencies of the same order of magnitude as the dipolar coupling interaction among protons, the Hartmann−Hahn (H−H) matching condition is split into several sideband-matching positions. The split matching features, resulting from the modulation effect of MAS on both the heteronuclear and homonuclear dipolar interactions, have been observed and analyzed in organic solids[25−27] and in zeolites.[24] Figure 1 shows the graphs of ^{1}H→^{29}Si cross-polarization transfer recorded at different spinning speeds.

Each graph presents the amplitude of the proton-enhanced silicon-29 NMR signal of $Q^{(3)}$ site in magadiite as a function of the amplitude of the rf field applied at the ^{29}Si frequency. As expected, in analogy to organic solids, under (fast) MAS the H−H matching position splits into several H−H mismatched sidebands separated by rf field difference equivalent to the spinning frequency. This visualizes well the fact that under fast

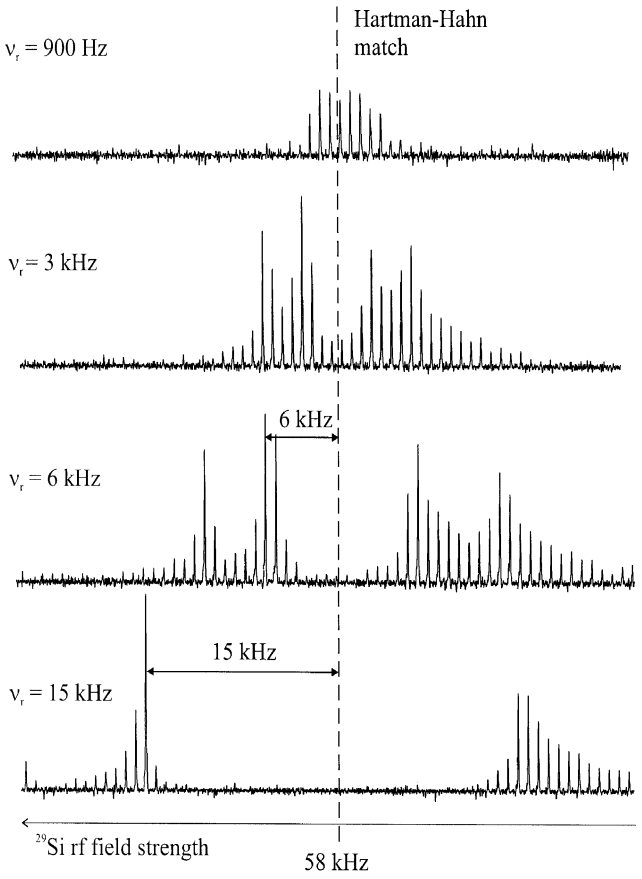

Figure 1. Hartmann−Hahn matching curves for $Q^{(3)}$ site in magadiite at different spinning speeds. The contact time period was 1 ms and the ^{1}H rf field strength was $\omega_{1I}/2\pi = 58$ kHz.

spinning, ^{1}H→^{29}Si CP occurs effectively only when the generalized H−H matching condition $\omega_{1H} = n\omega_r + \omega_{1Si}$ with $n = 1, 2,...$ is satisfied. According to the theory of CP under MAS, the H−H matching curve is predicted to be symmetric with respect to the center-matching condition. We attribute the observed asymmetry to the effect of rf field inhomogeneity, small resonance offsets and some instability of high power amplifications. The calculations reproducing satisfactorily the envelope of matching curves at different spinning frequencies give the heteronuclear dipolar coupling constant close to 1.4 kHz. This would correspond to a realistic internuclear ^{1}H−^{29}Si distance of 2.57 Å, indicating that the $Q^{(3)}$ resonance signal is largely dominated by efficiently polarizing sites having rigid OH groups. From Figure 1, it is clear that even a moderately high spinning rates are sufficient to cause the Hartmann−Hahn proton-silicon match condition to be very critical and inefficient so that only CP under mismatched conditions remains possible. However, it is difficult to achieve stable and reproducible results using mismatched H−H cross-polarization, because even very small (<0.1%) instability of rf fields may lead to an important loss of intensity of the NMR signal. Consequently, it may be necessary to search for methods which will render the cross polarization less sensitive to exact matching of the applied radio frequency field strengths, especially upon high spinning speeds. Several methods using amplitude or phase modulated rf have been proposed and applied in organic solids.[28−30] To our knowledge, none of them has been applied so far in the case of ^{1}H→^{29}Si polarization transfer. The results shown in Figure 2 indicate that the matching condition can be indeed substantially broadened by 180° phase shifts (Figure 2b) or variable-amplitude rf field CP transfer (Figure 2c,) and can even trim down the

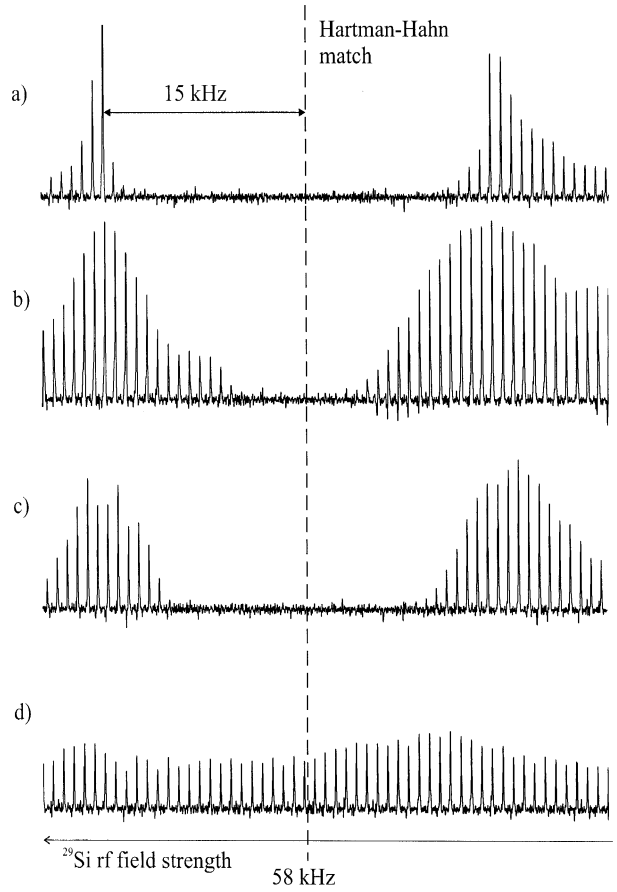

Figure 2. Cross-polarized intensity versus ^{29}Si rf field strength for $Q^{(3)}$ site in magadiite spinning at 15 kHz. (a) standard CP transfer; (b) phase-inverted (π phase shift every rotor period) ^{29}Si rf irradiation during CP; (c), (d) variable-amplitude CP using 15 amplitudes of ^{29}Si rf field increased in steps changing in the range 0.9−1.0 and 0.58−1.0, respectively. The total contact time period was 1 ms in each case.

burden of finding and maintaining an exact CP match (Figure 2d). This may be very useful in any experiment involving ^{1}H→^{29}Si polarization transfer and high spinning speeds.

We have taken advantage of less critical matching conditions upon the amplitude/phase modulated ^{29}Si rf field cross-polarization in the heteronuclear shift correlation experiments described below.

Simulations. All simulations presented in this paper have been performed using the homemade simulation program.

Results

^{1}H MAS Spectra. Proton NMR spectroscopy, an inherently quantitative, sensitive probe of the hydrogen environment, has been widely utilized to investigate the nature of hydrogen bonded systems, especially in systems of biological interest.[31] A large range of proton NMR chemical shifts of ca. 20 ppm is observed in solids for oxygen-bound hydrogens.[32] It has been also demonstrated theoretically[33] and experimentally[34,35] that the proton chemical shifts of oxygen-bond hydrogen show linear dependence on the O−H····O distance. Recent progress in the design of magic angle spinning (MAS) equipment allows that spinning frequencies of 15 kHz are now routinely available, and even higher frequencies up to 35 kHz are feasible with commercial probes. In solids with not very tightly coupled protons, such spinning frequencies are sufficient to efficiently remove the dipolar broadening, which results in highly resolved proton spectra. Figure 3 (left) shows ^{1}H MAS NMR spectra of magadiite acquired with spinning frequencies ν_r ranging from 5 to 15 kHz.

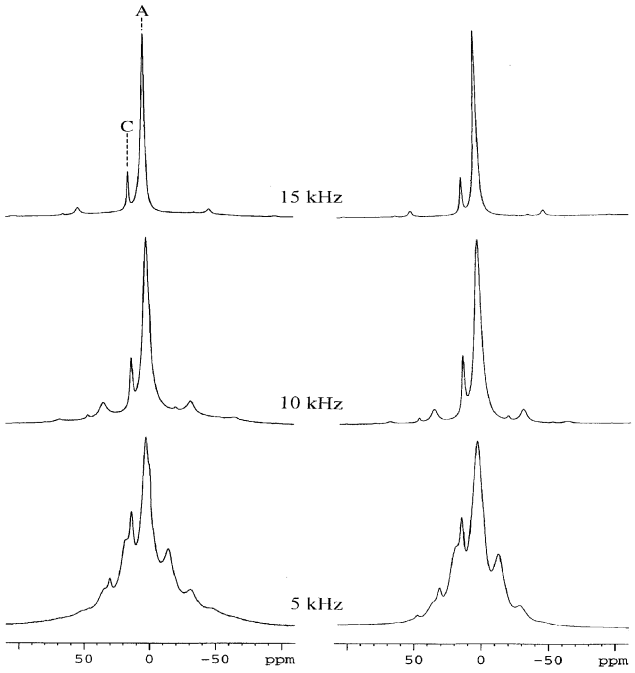

Figure 3. Experimental (left) and calculated (right) 300.13 MHz ^{1}H MAS spectra of magadiite at different spinning frequencies. A and C indicate two isotropic positions at δ_{iso} = 3.8 and 15.2 ppm, respectively. For simulation details see text.

TABLE 1: ^{1}H NMR Data for Hydrous Species in Magadiite

	δ_{iso} (ppm)	dip (kHz)	T_2 (s)	%	δ_{11}, δ_{22}, δ_{33} (ppm)	$T_{1\rho}^H$ (ms)
H_2O	3.8	10.0	$1.1-3.5 \times 10^{-4}$ (a)	89		0.4
OH	15.2	10.0	$2.8-5.5 \times 10^{-4}$ (a)	11	30.0, 30.0, −14.4	0.8

[a] Spinning speed dependent.

High-speed MAS leads to an efficient narrowing of the dipolar broadening permitting a clear resolution of two isotropic positions at δ_{iso}=3.8 (position A) and 15.2 ppm (position C). Similar proton shifts have been observed in natural samples of magadiite, makatite, kanemite, octosilicate, and kenyaite[18] and in the synthetic RUB-18.[6] The low field peak at 15.2 ppm represents evidently protons involved in hydrogen bonding, the high-field signal corresponds to the remaining hydrous species. In Figure 3 (right), we have presented simulations corresponding to the observed spinning sidebands manifolds. The theoretical spectra were calculated from the evolution of the proton dipolar interaction under MAS conditions. The overall appearance of the experimental spectra is well reproduced in the simulated spectra assuming a simple two spin system. The interactions with a greater number of neighboring protons lead to the homogeneous dipolar broadening which was accounted for in the corresponding T_2 relaxation times. Fitted values of residual dipolar couplings, spin−spin relaxation times, as well as the amount of each component are given in Table 1.

Figure 4 shows the ^{1}H MAS spectra of progressively rehydrated, initially vacuum-dried (a) magadiite sample, the latter spectrum being dominated by the presence of a narrow and a relatively broad resonance signal, the narrow centered at 10.2 ppm (B position), the broad one expanding between 0 and 15 ppm.

Double-Quantum ^{1}H MAS Experiments. Multiple-quantum (MQ) spectroscopy is now used routinely in liquid NMR to filter

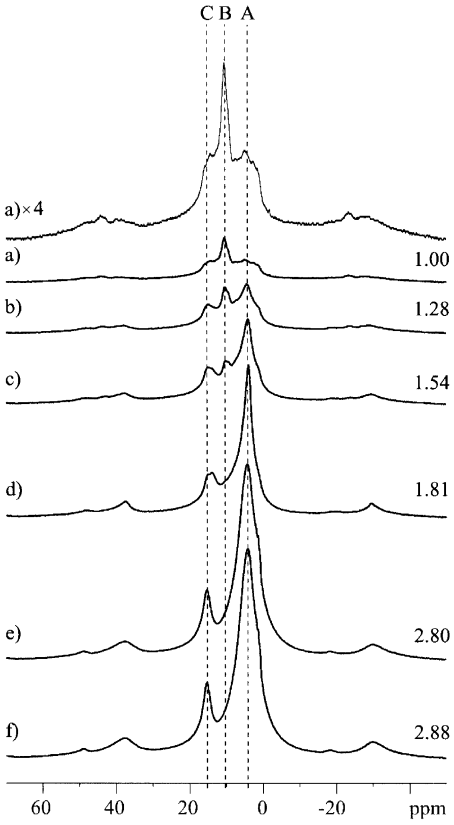

Figure 4. ^{1}H MAS spectra of progressively rehydrated, initially vacuum-dried (a) magadiite sample spinning at 10 kHz. The spectra were recorded with rehydration times: (b) 15 min; (c) 25 min; (d) 40 min; (e) 13 h; and (f) 57 h. Integrated intensity in each case is also indicated. Position B indicates isotropic chemical shift at δ_{iso}=10.2 ppm. The assignment of the peaks is discussed in the text.

out the transitions arising from groups of coupled spins and thereby to simplify the resulting spectra.[20] In solids and liquid crystals, MQ experiments have been used most frequently for studies of clustering and molecular conformations.[36] The excitation of MQ coherences via dipole−dipole couplings in the presence of fast MAS permits to take advantage of high resolution and sensitivity enhancement. Restricting the MQ excitation to double-quantum (DQ) order, the dipolar coupled systems can be analyzed in a pairwise manner[37] with respect to the chemical shifts of the involved nuclei.[38] In our case, we expect to clarify in this manner the local dipolar environment of the hydrogen species present in magadiite. Figure 5 shows the proton 2D spectrum of magadiite, together with the double-quantum projection ω_1 and the single-quantum projection ω_2.

As the DQ peak intensity is inversely proportional to a power six of the distance between dipolar coupled protons,[37] by simple inspection of which peaks are present or absent in this spectrum, direct visualization of the proton−proton proximities is immediately available. Apart from the expected presence of an auto peak of water molecules appearing at 3.8 and 7.6 ppm at the single- and double-quantum chemical shift scale, respectively, an off-diagonal peak clearly shows a spatial proximity of protons appearing at 3.8 and 15.2 ppm. Contrary, the absence of an auto 15.2/30.4 ppm peak, even when using dipolar recoupling sequences, indicates definitely that there is no close proximity of the hydrogen bonded hydroxyl groups and that water hydrogens are neither concerned by hydrogen bonding. This means that the hydrogen bonding involves either the oxygen of an another $Q^{(3)}$ tetrahedra from the same or neighboring layer or the water oxygen.

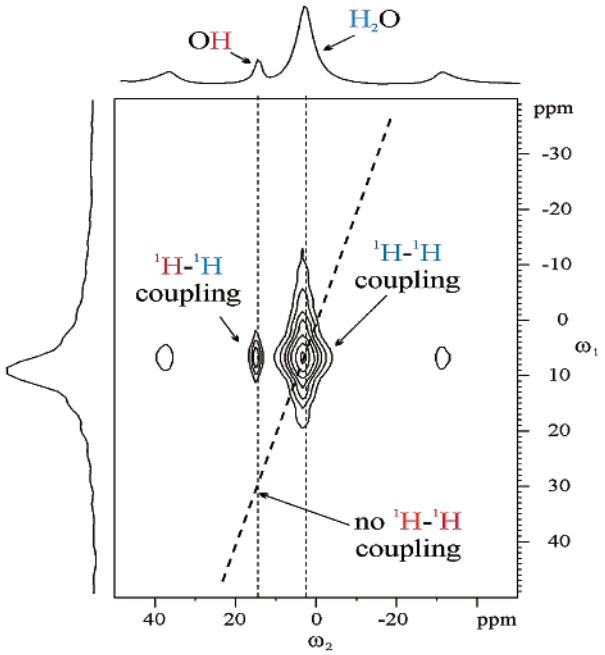

Figure 5. ^{1}H double-quantum MAS NMR spectrum, together with skyline single-quantum (ω_2) and double-quantum (ω_1) projections of magadiite spinning at 15 kHz.

^{2}H MAS Spectroscopy. Deuterium NMR is a powerful method for studying molecular mobility in solids.[39] For low molar mass fluids, the deuterium NMR spectrum is a single narrow line due to rapid isotropic molecular motions that average out quadrupolar broadening. Conversely, in the presence of fast anisotropic motions, the quadrupolar interaction is only partially averaged, to an extent depending on the geometry of molecular dynamics. Deuterium MAS NMR spectra can be obtained with quality suitable for quantitative analysis in relatively short accumulation times. This is due to the magic-angle spinning effect that dramatically increases the sensitivity of ^{2}H NMR spectra by breaking up the broad quadrupolar powder pattern into a family of sharp spinning sidebands. The room temperature ^{2}H MAS spectrum of deuterium exchanged magadiite is shown in Figure 6.

Two sets of quadrupolar spinning sidebands indicate clearly the presence of two components with differing motional behavior. On the basis of their chemical shift difference equal to 11.4 ppm, and corresponding exactly to that observed in ^{1}H MAS spectra, we assign the low field, Pake-like spinning sidebands envelope to the hydrogen bonded species. The high field, much more restricted manifold of relatively large spinning sidebands, is due to remaining more mobile species not involved in the hydrogen bonding. We were able to obtain satisfactory agreement between experimental and simulated deuterium MAS spectrum by a superposition of two spectral components characterized by distinct quadrupolar constants (e^2Qq_{ZZ}/h) and quadrupolar asymmetry parameters (η) along with their associated proportions (see Table 2).

^{1}H−^{29}Si and ^{1}H−^{23}Na HETCOR Experiments. As visible in Figure 3, fast MAS permits us to obtain well-resolved chemical-shift proton spectra of magadiite without a simultaneous application of homonuclear decoupling. This is possible due to the inhomogeneous character of line broadening resulting from weakly coupled proton spin system. On the other hand, as discussed above, high-resolution ^{29}Si spectra of magadiite can be acquired by using appropriate experimental conditions for cross-polarization transfer upon magic angle spinning. Figure

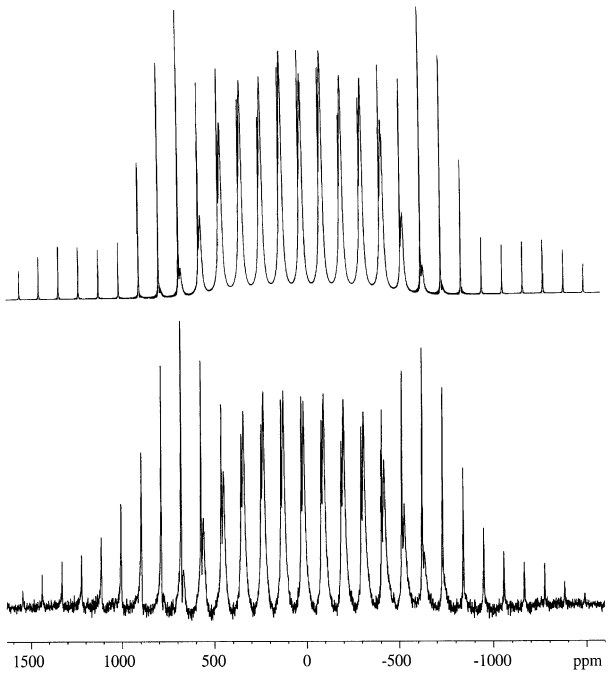

Figure 6. Experimental (bottom) and calculated (top) ^{2}H MAS spectrum of deuterium-exchanged magadiite sample spinning at 5 kHz. For simulation details see text.

TABLE 2: ^{2}H NMR Data for D_2O Exchanged Magadiite

	δ_{iso} (ppm)	e^2Qq_{zz}/h (kHz)	η	T_2(s)	%
D_2O	3.8	29.0	~0.9	$5.0\ 10^{-3}$	87
OD	15.2	77.0	~0.0	$4.0\ 10^{-4}$	13

7 (left) presents static and MAS cross-polarization ^{29}Si spectra of magadiite.

The static spectrum shows a relatively narrow signal centered near −110 ppm and a relatively broad powder pattern of axial symmetry with a width of about 80 ppm. Due to a much more symmetric electronic environment of $Q^{(4)}$ sites, the narrow and broad powder patterns are assigned to $Q^{(4)}$ and $Q^{(3)}$ tetrahedra, respectively. According to previously reported ^{29}Si MAS spectra[3], a single resonance signal at −99.7 ppm, and three peaks between −110.2 and −114.0 ppm represent the isotropic chemical shifts of $Q^{(3)}$ and $Q^{(4)}$ units, respectively. From the fully relaxed, single pulse (repetition rate 4000s), fast MAS spectra ($\nu_r = 10$ kHz), the integrated intensity ratio $Q^{(3)}$:$Q^{(4)}$ of our sample is equal to 1:2.6. The same ratio is calculated for vacuum-dried sample despite considerable broadening of resonance signals. We wish to point out that in both static as well as magic-angle spinning CP spectra in Figure 7(left), the $Q^{(4)}$ sites appear with an underrepresented intensity as compared with $Q^{(3)}$ units. Figure 7 (right) shows ^{23}Na single pulse spectra of static and spinning sample recorded at 79.4 MHz. The appearance of only one, narrow signal without visible second order quadrupolar broadening suggests the presence of a single sodium site with a symmetric, most probable octahedrally coordinated environment.[16,17]

As two distinct proton signals are present, it is interesting to know if both corresponding hydrous species participate in the polarization transfer to the ^{29}Si and ^{23}Na nuclei. This in turn would allow getting independent structural and/or dynamic information. Such an information can be obtained from the two-dimensional ^{1}H−^{29}Si correlation experiment employing the CP procedure.[24,40] We have used this experiment with three modifications, two of them consisting in employing during the evolution period the rf irradiation at the resonance frequency

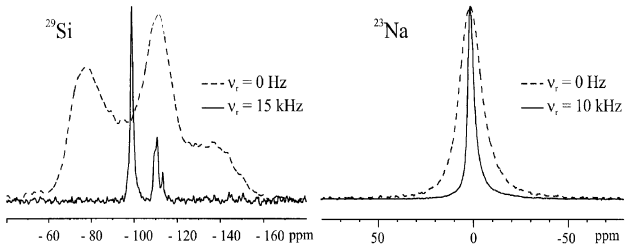

Figure 7. ^{29}Si cross-polarization (left) (contact-time of 3 ms) and ^{23}Na single pulse (right) static and magic-angle spinning spectra of magadiite.

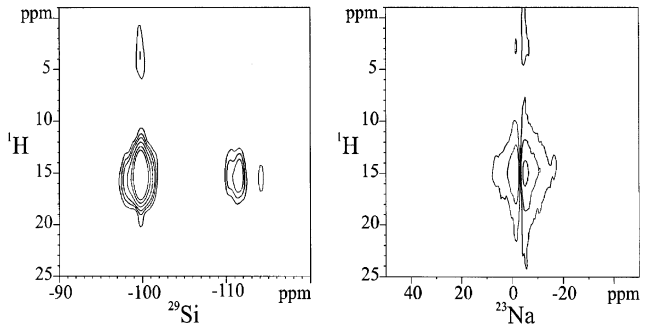

Figure 8. ^{1}H−^{29}Si (left) and ^{1}H−^{23}Na (right) HETCOR spectra of magadiite obtained using CP contact time of 3 and 0.5 ms, and spinning speeds close to 15 and 6 kHz, respectively. Phase-modulated CP has been used for optimal conditions of magnetization transfer (see experimental part).

of S (^{29}Si or ^{23}Na) nuclei, and the proton decoupling during the acquisition. This eliminates possible heteronuclear dipolar effects[41] in each spectral dimension which may not be totally canceled at moderate magic-angle spinning speeds. The third modification consisted of applying the phase modulated rf field during the cross-polarization period (see the Experimental section), which permitted us to maintain the required stability in the magnetization transfer at high spinning speeds.

^{1}H−^{29}Si and ^{1}H−^{23}Na heteronuclear shift correlation (HETCOR) spectra carried out on magadiite are shown in Figure 8.

Somewhat surprisingly, especially in the case of proton−sodium correlation, strong heteronuclear connectivities involve mainly the minor proton peak appearing at 15.2 ppm. Similar results have been reported earlier for octosilicate,[42] RUB-18[6] and for dried natural magadiite.[12] In our case of fully hydrated sample, this means that despite the 8-fold higher amount of hydrous species appearing at 3.8 ppm, the hydrogen-bonded species are still the most efficient sites for CP magnetization transfer. However, it does not mean that these hydrogen-bonded protons constitute the principal source of nuclear magnetization, whereas the remaining hydrous species are not able to participate significantly in the polarization transfer. We will come back to this important point in the next part. We also wish to point out that the observed small intensity connectivities involving hydrous species appearing at 3.8 ppm are not due to the effect of proton spin exchange (spin diffusion or chemical exchange). In fact, as checked by us in independent homonuclear one and two-dimensional correlation experiments, such process does not occur for magadiite on the time scale of these experiments in conditions of fast magic angle spinning and short CP contact time.

We have taken advantage of the observed selective cross-polarization from hydrogen bonded groups by recording the HETCOR spectra of magadiite at relatively low spinning speeds. This permitted us to get information about the chemical shift anisotropy tensor of hydrogen bonded groups, information which

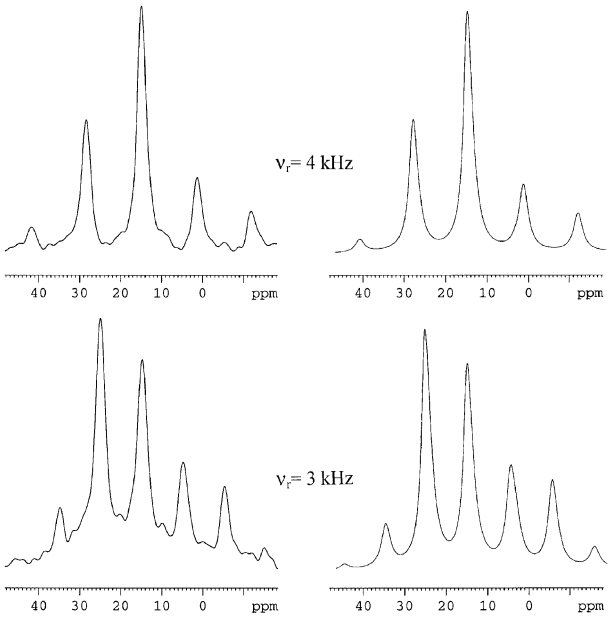

Figure 9. Experimental (left) cross-sections extracted from the $^{1}H-^{29}Si$ HETCOR spectra at 15.2 ppm on the proton chemical shift scale along with the fitted (right) proton CSA spectra at two different spinning speeds.

was unreachable from the single pulse ^{1}H MAS spectra due to the presence of the resonance signal at 3.8 ppm (Figure 3). The corresponding cross-sections extracted from the $^{1}H-^{29}Si$ 2D shift correlation spectra, along with the simulated CSA spectra are shown in Figure 9.

Very similar cross-section envelope of spinning sidebands, albeit containing substantial bump-like contribution from signal at 3.8 ppm, was also observed in the $^{1}H-^{23}Na$ shift correlation experiment carried out at the same spinning speed.

$^{1}H\rightarrow^{29}Si$ and $^{1}H\rightarrow^{23}Na$ Cross-Polarization Dynamics. Our principal motivation for the investigation of CP dynamics was to understand structural and dynamic features responsible for the unusual, largely selective transfer of magnetization from hydrogen bonded hydroxyl groups, as shown above by heteronuclear shift correlation experiments. So far, no CP dynamics studies have been reported for the layered hydrous silicates. It is well-known that in order to reduce the measurement time and to increase the sensitivity, the NMR signal of rare S nuclei with low gyromagnetic ratio γ can be acquired in solids by using cross-polarization with abundant I nuclei having high γ, such as protons.[22] The CP spin dynamics can be understood as a thermodynamic equilibration between the thermal reservoirs of the two spin systems I and S. Assuming that there is no relaxation of the S spins, the NMR signal of these spins, as a function of contact time t_{CP}, can be described by the well-known relationship[43]

$$M_S(t_{CP}) = M_S^{\infty}\alpha\frac{\gamma_I}{\gamma_S}\frac{1}{1-\dfrac{T^{IS}}{T_{1\rho}^{I}}}\left(\exp\left(-\frac{t_{CP}}{T_{1\rho}^{I}}\right)-\exp\left(-\frac{t_{CP}}{T^{IS}}\right)\right) \quad (1)$$

where M_S^{∞} is the equilibrium magnetization of spins S; $\alpha = \omega_{1I}/\omega_{1S} = (\gamma_I H_{1I})/(\gamma_S H_{1S})$ is the ratio of the radio frequency fields at the I and S frequencies (the Hartman−Hahn mismatch parameter, usually $\alpha = 1$); $1/T^{IS}$ is the cross-polarization rate, which increases dramatically with the strength of the heteronuclear I−S dipolar interaction but also depends in a complex way on the strength of the homonuclear I−I dipolar interaction between the abundant spins, on the correlation time of molecular motions and on the experimental parameters; $T^{I}_{1\rho}$ is the relaxation time in the rotating frame of the I spins. According to eq 1, the CP build up curves are inherently sensitive to internuclear distances via T^{IS} and the presence of mid-kHz motions via $T^{I}_{1\rho}$, this makes that the dynamics of CP transfer still remain one of the most attractive NMR tools for structural and motional investigation of solids.

As has been pointed out very recently,[44] the expression 1 is valid not only when $T^{IS} < T^{I}_{1\rho}$, the usual condition (fast CP regime), but also holds whatever the ratio $T^{IS}/T^{I}_{1\rho}$. NMR cross-polarization measurements are usually analyzed assuming that the cross-polarization time T^{IS} of magnetization transfer from the abundant I spins to the rare S spins is shorter than the relaxation time $T^{I}_{1\rho}$. However, the reverse situation (i.e., $T^{IS} > T^{I}_{1\rho}$, slow CP regime) may be encountered, especially in inorganic solids where protons are more remote from rare nuclei than in organic systems. In this case, the S spin magnetization will as well begin to rise but this increase cannot proceed further when the I spin system is rapidly depleted by the $T^{I}_{1\rho}$ relaxation. Consequently, the transfer of magnetization is stopped at a time close to $T^{I}_{1\rho}$ and there is a reverse flow from the S to I spin system which remains depleted by the faster $T^{I}_{1\rho}$ relaxation. This reverse flow from the S to the I reservoir occurs, as does the forward one, at the cross-polarization rate $1/T^{IS}$. In such a situation, when analyzing the experimental data under the usual fast CP assumption, an interpretation of both dynamic parameters will be strongly in error. In fact, it is impossible to know from the cross-polarization curve alone, whether $T^{IS} < T^{I}_{1\rho}$, or $T^{IS} > T^{I}_{1\rho}$. This is the consequence of the fact, that apart from the intensity factor, eq 1 is fully symmetrical with respect to the interchange of T^{IS} and $T^{I}_{1\rho}$.

Contrary to the standard variable-contact CP experiment, a direct visualization of the ratio $T^{IS}/T^{I}_{1\rho}$ is easily accessible by using the TORQUE experiment.[23] This experiment has been originally designed with the aim of quenching the I spin $T^{I}_{1\rho}$ dependence (**T O**ne **R**ho **QUE**nching) when studying polarization transfer in solids with $T^{IS} < T^{I}_{1\rho}$. It uses a spin lock period on spin I of duration t_{SL} followed by the CP transfer of variable duration t_{CP}, the total time $T_{TORQUE} = t_{CP} + t_{SL}$ being kept constant. The TORQUE signal grows as a function of t_{CP} according to

$$M_S^{TORQUE}(t_{CP}) = \exp(-T_{TORQUE}/T_{1\rho}^{I})\left(\frac{1-\exp(-(1-\lambda)(t_{CP}/T^{IS}))}{(1-\lambda)}\right) \quad (2)$$

with $\lambda = T^{IS}/T^{I}_{1\rho}$. Figure 10 shows the simulations of the temporal evolution of S spin magnetization in a standard CP experiment and in the TORQUE experiment, both in three different situations: (i) $T^{IS} < T^{I}_{1\rho}$; (ii) $T^{IS} > T^{I}_{1\rho}$; (iii) a simple combination of (i) and (ii) cases.

As expected, in the standard CP experiment, apart from the differences in the absolute intensity, identical temporal evolution of magnetization is observed in each case. However, dramatic differences in the curvature of the TORQUE temporal evolution are visible. This permits us an unambiguous recognition of the $T^{IS}/T^{I}_{1\rho}$ ratio and ensures the proper analysis of dynamic CP parameters in terms of structural and/or motional features.

The experimental build up curves obtained from standard CP and TORQUE experiments for $Q^{(3)}$ and Na^{+} are shown in Figure 11.

Assuming as usual that $T^{IS} < T^{I}_{1\rho}$, the standard CP curves can be fitted according to eq (1), each of them being described

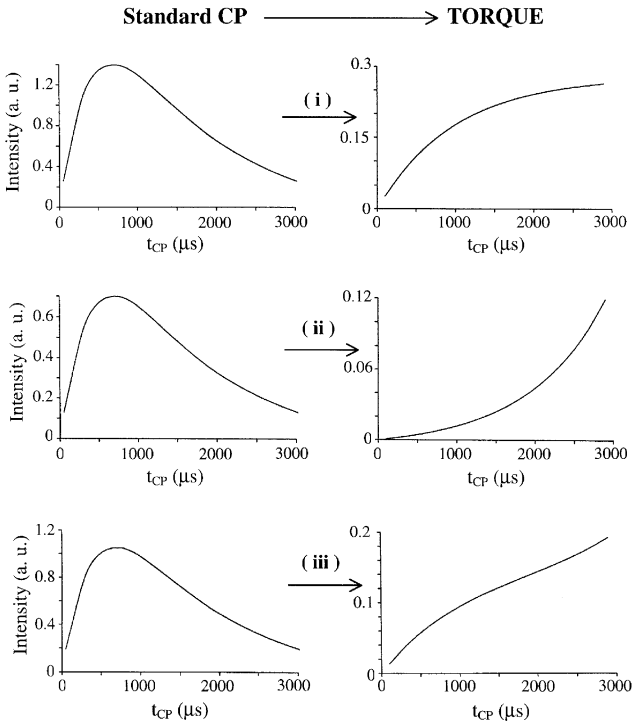

Figure 10. Magnetization transfer time dependence in standard CP (left) and TORQUE (right) experiments calculated using eqs 1 and 2 with (i) $T^{IS} = 0.5$ ms, $T^{I}_{1\rho} = 1.0$ ms; (ii) $T^{IS} = 1.0$ ms, $T^{I}_{1\rho} = 0.5$ ms; (iii) equally weighted (i) plus (ii) conditions.

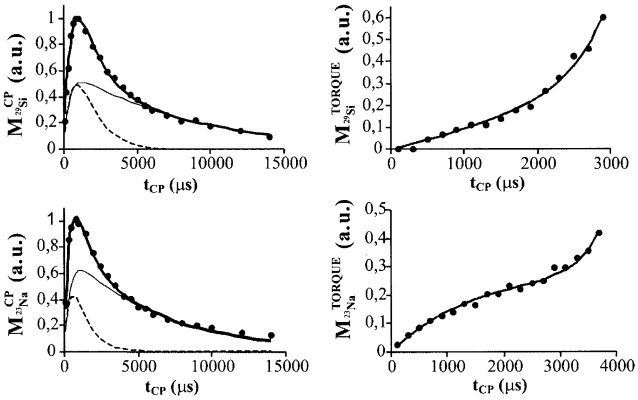

Figure 11. Temporal evolution of ^{29}Si (top) and ^{23}Na (bottom) magnetization in the standard CP (left) and TORQUE (right) experiments for $Q^{(3)}$ and Na^+ sites of magadiite spinning at 3 kHz.. Solid lines correspond to the fitted curves, fitted parameters are given in Table 1.

by two pairs of time constants T_{up} and T_{down} for their rising and decreasing parts, respectively. A simple model for which each site is characterized by a single set of T_{up} and T_{down} values was found to be inadequate. However, the observed curvature in the TORQUE temporal dependence makes it immediately evident that it is essentially the $T^{IS} > T^{I}_{1\rho}$ situation which takes place for $Q^{(3)}$ sites. For Na^+ ions, the situation is even more complex, the TORQUE curve exhibits a pronounced S-shape form which means that both the fast and the slow CP regime are relevant for this CP dynamics. From the independent measurements of relaxation in the rotating frame, two distinct $T^{I}_{1\rho}$ values have been obtained for protons appearing at 3.8 and 15.2 ppm, respectively (see Table 1). It turns out that these two relaxation times are equal neither to T_{down} nor to T_{up} found in the fitting procedure of CP build up curves when assuming $T^{IS} < T^{I}_{1\rho}$. As the $T^{I}_{1\rho}$ values reflect two different proton environments existing in magadiite, a realistic model should include both relaxation parameters and assume at least two types of $Q^{(3)}$ as well as sodium sites being differently coupled to hydrogen species. Consequently, the CP and TORQUE build up curves are each the weighted sums of two different contributions, each one given by eqs (1) and (2) for CP and TORQUE, respectively. A good agreement between experimental and calculated CP and TORQUE temporal dependencies is indeed observed for both species under such assumptions. The fitted T^{IS} and corresponding proportions are given in Table 3.

TABLE 3: Analysis of Cross-polarization Dynamics in Magadiite

site	T^{IS} (ms)	$T_{1\rho}{}^{I}$ (ms)	%
$Q^{(3)}$	1.0	0.8 (b)	11
	8.0	0.4 (b)	89
$Q^{(3)}$ (a)	0.4	2.0 (b)	31
	4.0	25.0 (b)	69
Na^+	0.5	0.8 (b)	8
	6.0	0.4 (b)	92

[a] Vacuum-dried sample. [b] Independently measured in direct and/or indirect proton $T_{1\rho}$ experiments.

The ensemble of fitted dynamic parameters makes it now clear the reasons for largely selective cross-polarization transfer involving the hydrogen-bonded hydroxyl groups, as observed in both heteronuclear correlation experiments, and brings evidence that the long time decays of magnetization in the standard CP experiments result from the back flow of magnetization to the proton system.

Discussion

Hydrogen Bonding Nature. The presence of hydrogen bonding has been reported for sodium polysilicates by different authors.[12,15,18,19,45] The interlayer character of hydrogen bonding involving the silanol groups has been first proposed by Almond and co-workers.[18] Another model of the intercalated water molecules linked via hydrogen bridges to the silanol groups of the two adjacent silicate layers in RUB-18 has been proposed by Vortmann et al.[45] Very recently, Eypert−Blaison et al.[19] suggested that in magadiite the water molecules rather than silanol groups are present in a "strongly hydrogen bonded state". However, the inspection of MAS spectra in Figure 3 indicates that only protons appearing at 15.2 ppm are hydrogen bonded and that the water hydrogens are not involved in any strong hydrogen bonding. Indeed, the DQ spectrum shown in Figure 5 definitely proves that water molecules are represented only by the resonance signal at 3.8 ppm. The position of this signal reveals the upfield shift of 1.0 ppm with respect to the resonance signal of liquid water, which reflects rather weak if any hydrogen bonding of water hydrogens.[34,35] Using the relationship of Eckert and co-workers,[34] the isotropic chemical shift of 15.2 ppm corresponds to the O−H···O distance of ca. 2.5 Å. This relatively short distance is consistent with strong hydrogen bonding of hydroxyl groups.

These results corroborate well with the large chemical shift anisotropy $\Delta\delta = -44.4$ ppm obtained for the 15.2 ppm signal from the low-speed heteronuclear shift correlation experiments (Figure 9). It is known that the chemical shift tensor is a sensitive measure of hydrogen bonding that can yield more information than the isotropic shift alone.[31,32] For hydrogen bonded hydroxyl protons, the proton shielding is close to axially symmetric with the symmetry axis of the tensor (the most shielded axis) close to parallel to the O−H direction.[46] On the basis of the correlation of the proton chemical shift tensor anisotropy with the O−H···O

distance,[33] the fitted axially symmetric tensor from spectra in Figure 9 corresponds indeed very well to the 2.5 Å ± 0.05 distance.

^{2}H MAS spectrum of deuterium labeled magadiite shown in Figure 6 provides another independent evidence of the strong hydrogen bonding character of the hydroxyl groups. From the simulation of the deuterium spinning sideband manifold imitating Pake like doublet, a quadrupolar coupling constant (qcc) of 77 kHz has been obtained. On the other hand, the fitted quadrupolar asymmetry parameter η value reveals a rigid character of the OD groups. These results are consistent with the well-known fact that the deuterium quadrupolar coupling constant decreases dramatically upon hydrogen-bond formation.[47] In analogy to the relationship between proton chemical shift and the strength of hydrogen bonding, a dependence of the ^{2}H qcc upon O−H····O distance has been indeed found experimentally and theoretically.[47] According to this dependence, the fitted qcc corresponds to the O···O distance of 2.5 ± 0.05 Å, which is remarkably similar to that found from proton chemical shift dependence. This is indeed an another strong indication that protons appearing at 15.2 ppm can be considered as rigid species on the NMR time scale of 10^{-5} s.

Concerning an important issue of the structural character of hydrogen bonding, the comparison of the ^{1}H MAS spectra of hydrated and vacuum-dried magadiite, as well as of progressively rehydrated samples (Figure 4), gives strong evidence against the presence of the interlayer hydrogen bonding of silanol groups. In fact, beside the expected disappearance of the resonance signal at 3.8 ppm (A position), a 5.0 ppm upfield shift of the resonance position of OH groups is observed in the vacuum-dried sample (B position). According to the relationship of Eckert et al.,[34] such a shift corresponds to increasing O−H····O distance by ca. 0.2 Å which in the case of interlayer hydrogen bonding seems to be quite incompatible with the 3−4 Å change of the basal spacing when going from the hydrated to the dehydrated sample of magadiite. It is indeed most unlikely that the interlayer hydrogen bonding could survive after the vacuum dehydration leading to 15−20 times higher change of the basal distance as compared with the observed change of the O−H····O distance. This prompts us to think rather about the intralayer hydrogen bonding taking place between neighboring tetrahedra. In this case, the observed 0.2 Å change of the O−H····O distance between vacuum-dried and fully hydrated can be easily explained by small changes in the mutual orientation of neighboring tetrahedra. Another possible explanation for the change of the isotropic position during the removal of intercalate water would be due to the increasing effect of charge of Na^+ upon the proton chemical shift.

Additional observation supporting the presence of the intralayer hydrogen bonding between neighboring tetrahedra comes from the small line-widths of proton resonance signals at 10.2 and 15.2 ppm and from the ^{2}H spinning sidebands pattern envelope, giving evidence against both broad distribution of isotropic chemical shifts and quadrupolar coupling constants of hydroxyl groups. Indeed, in the absence of a long range order, a broad distribution of both parameters resulting from a broad range of interlayer O−D····O distances would be expected. Concerning the state of the remaining water in a vacuum-dried sample (roughly three out of four water molecules have been removed in the vacuum-dried sample), the presence of a relatively broad resonance signal centered about 9−10 ppm (see Figure 4a′) and double-quantum experiments (not shown) give obvious evidence for tightly coupled, hydrogen bonded network. This is confirmed by a slowing down of $T_{1\rho}$ relaxation of proton

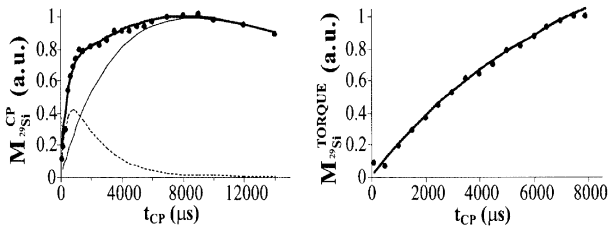

Figure 12. Time dependence of the ^{29}Si magnetization for $Q^{(3)}$ site of vacuum-dried sample of magadiite spinning at 3 kHz in the standard CP (left) and TORQUE (right) experiment. Solid lines correspond to the fitted curves (see also Table 1).

reservoir, as visualized in Figure 12 by the cross-polarization build-up curve and the TORQUE temporal dependence that clearly switched out to the fast CP regime.

Motional Features of Interlayer Water. Although narrowing of the static proton line-width upon MAS indicates that the motion of the water molecules does not involve rapid, isotropic reorientations, the weakness of the spinning sidebands associated with the proton signal at 3.8 ppm in Figure 3 and the fitted residual dipolar coupling value suggests the presence of significant mobility of the interlayer water protons on the NMR time scale. In fact, the water molecules present in hydrous crystals and undergoing solely fast anisotropic 180° flips show the spinning sideband patterns extending over a 100 kHz range.[35,48] For magadiite, the proton−proton dipolar interaction within water molecules is roughly 4-fold reduced by fast molecular motion involving a higher degree of internal mobility. This is confirmed by the presence of motionally averaged deuterium spinning sidebands manifold with a residual quadrupolar coupling constant of 29 kHz. As the qcc for static D_2O coordinated to Na^+ is expected to be ca. 250 kHz,[49] the observed reduction of qcc confirms substantial motional freedom of the interlayer water rotating at rates which are rapid on the NMR time scale (10^{-5}s). This corroborates well with the small efficiency of magnetization transfer from water molecules, as clearly visualized by cross-polarization and heteronuclear shift correlation experiments.

One can wonder what kind of molecular motion is responsible for the shape of the envelope of quadrupolar spinning sidebands manifold. Figure 6 shows that the experimentally observed envelope can be satisfactorily fitted by an effective quadrupolar coupling tensor with asymmetry η equal to 0.9. Assuming the presence of a single axial motion, the effective tensor is oriented such that its unique axis lies parallel to the rotation axis and the residual quadrupolar coupling constant is $\langle qcc \rangle = qcc1/2(3\cos^2\theta - 1)$. This permits us to estimate the angle θ between the principal z axis of the static quadrupolar tensor (being roughly parallel to the O−D axis) and the motional axis which in our case takes the values of 59° (or 50°). This would correspond to the water molecules rotating roughly about the D−O−D bisecting axis which itself may be expected to be parallel to the Na^+−O axis. However, we wish to point out that the detailed information about the mechanism and rates of motional processes of water, which may also involve a combination of rapid axial motion and a multiple-site jump exchange, will need to go further into the analysis of ^{2}H NMR line shapes recorded in a large temperature range.

Conclusions

We have obtained new information about structural and motional features of magadiite, a layered sodium silicate hydrate, by choosing complementary ^{1}H, ^{2}H, ^{29}Si, and ^{23}Na NMR methodologies.

Fast ^{1}H MAS permitted to distinguish and quantify different chemical environments of hydrous species, single-and double-quantum MAS spectra revealed the intralayer rather than interlayer hydrogen bonding of hydroxyl groups. The measured ^{2}H quadrupolar coupling constant of hydrogen bonded species corresponds to the O−H····O distance of 2.5 ± 0.05 Å which is remarkably similar to that found from proton isotropic chemical shift value as well as from the anisotropy of the proton chemical shift tensor. After submission of this paper, we learned of similar concept of the hydrogen bond between the neighboring Si−OH and Si−O$^-$ groups within Na−RUB-18.[50]

The present study also shows that the proper analysis of the ^{1}H→^{29}Si and ^{1}H→^{23}Na cross-polarization dynamics can provide new insights into the structure and mobility of the interlayer space. Two types of Q$^{(3)}$ tetrahedra, hydrogen-bonded silanols Si−O··H··O−Si and Si−O$^-$ type sites "feeling" the presence of water molecules have been distinguished by their different ability to cross-polarize and different mobility of neighboring hydrous species. Although a unique, relatively narrow resonance ^{23}Na NMR signal is observed in single-pulse spectra, the cross-polarization dynamics clearly reveals the existence of at least two different sites for sodium ions, some of them "seeing" preferentially water molecules, the remaining "feeling" firmly the presence of hydroxyl protons involved in the hydrogen bonding.

Deuterium spinning sidebands manifold confirms substantial motional freedom of the interlayer water with the rates being rapid on the NMR time scale (10^{-5}s). The residual quadrupolar coupling constant would correspond to the water molecules rotating roughly about the D−O−D bisecting axis.

We believe that the strategy applied in this work might as well be useful to obtain deeper insight into structural and motional features of related alkali metal layered polysilicates and of other classes of nanoporous materials.

Acknowledgment. We thank D. Heidemann, Centre of Inorganic Polymers, Berlin, for making available for us the silicon-29 T_1 relaxation time measurements on natural and synthetic magadiite samples and C. Eypert-Blaison, INPL-ENSG, Nancy, for her generous gift of magadiite sample used in this work. We also thank C. Exley and C. Schneider, Keele University, for reading the manuscript.

References and Notes

(1) Eugster, H. P. *Science* **1967**, *157*, 1177.
(2) Lagaly, G.; Beneke, K.; Weiss, A. *Am. Miner.* **1975**, *60*, 642.
(3) Schwieger, W.; Heidemann, D.; Bergk, K.-H. *Rev. Chim. Miner.* **1985**, *22*, 639.
(4) Annehed, H.; Fälth, L.; Lincoln, F. J. *Z. Kristallogr.* **1982**, *159*, 203.
(5) Gies, H.; Marler, B.; Vortmann, S.; Oberhagemann, U.; Bayat, P.; Krink, K.; Rius, J.; Wolf, I.; Fyfe, C. A. *Microporous and Mesoporous Mater.* **1998**, *21*, 183.
(6) Wolf, I.; Gies, H.; Fyfe, C. A. *J. Phys. Chem.* B **1999**, *103*, 5933.
(7) Rojo, J. M.; Ruiz-Hitzky, E.; Sanz, J. *Inorg. Chem.*, **1988**, *27*, 2785.
(8) Fudala, A.; Konya, Z.; Kiyozumi, Y.; Niwa, S.-I.; Toba, M.; Mizukami, F.; Lentz, P. B.; Nagy, J.; Kiricsi, I. *Micropor. Mesopor. Mater.* **2000,** *35*−*36*, 631
(9) Brindley, G. W. *Am. Miner.* **1969**, *54*, 1583.
(10) Kosuge, K.; Yamazaki, A.; Tsunashima, A.; Otsuka, R. *J. Ceram. Soc. Jap.* **1992**, *100*, 738.
(11) Pinnavaia, T. J.; Johnson, I. D.; Lipsicas, M. *J. Solid State Chem.* **1986**, *63*, 118.
(12) Almond, G. G.; Harris, R. K.; Graham, P. *J. Chem. Soc. Chem. Commun.* **1994**, *7*, 851.
(13) Dailey, J. S.; Pinnavaia, T. J.*J. Inclusion Phenom. Mol. Recognit. Chem.* **1992**, *13*, 47.
(14) Heidemann, D. poster, *11th International Meeting on NMR Spectroscopy, Swansea*, 1993.
(15) Huang, Y.; Jiang, Z.; Schwieger, W. *Chem. Mater.* **1999**, *11*, 1210.
(16) Almond, G. G.; Harris, R. K.; Franklin, K. R.; Graham, P. *J. Mater. Chem.* **1996**, *6*, 843.
(17) Hanaya, M.; Harris, R. K. *J. Mater. Chem.* **1998**, *8*, 1073.
(18) Almond, G. G.; Harris, R. K.; Franklin, K. R. *J. Mater. Chem.* **1997**, *7*, 681.
(19) Eypert-Blaison, C.; Sauzéat, E.; Pelletier, M.; Michot, L. J.; Villiéras, F.; Humbert, B. *Chem. Mater.* **2001**, *13*, 1480.
(20) Ernst, R. R.; Bodenhausen, G.; Wokaun, A. *Principles of Nuclear Magnetic Resonance in One and Two Dimensions*, Clarendon, Oxford, 1987.
(21) Schnell, I.; Lupulescu, A.; Hafner, S.; Demco, D. E.; Spiess, H. W. *J. Magn. Reson.* **1998**, *133*, 61.
(22) Pines, A.; Gibby, M. G.; Waugh, J. S. *J. Chem. Phys.* **1973**, *59*, 569.
(23) Tekely, P.; Gérardy, V.; Palmas, P. Canet, C.; Retournard, A. *Solid State NMR* **1995**, *4*, 361.
(24) Vega, A. J. *J. Am. Chem. Soc.* **1988**, *110*, 1049.
(25) Stejskal, E. O.; Schaefer, J.; Waugh, J. S. *J. Magn. Reson.* **1977**, *28*, 105.
(26) Sardashti, M.; Maciel, G. M. *J. Magn. Reson.* **1987**, *72*, 467.
(27) Engelke, F.; Kind, T.; Michel, D.; Pruski, M.; Gerstein, B. C. *J. Magn. Reson.* **1991**, *95*, 286.
(28) Barbara, T. M.: Williams, E. H. *J. Magn. Reson.* **1992**, *99*, 439.
(29) Peersen, O. B.; Wu, X.; Kustanovich, I.; Smith, S. O. *J. Magn. Reson.* A **1993**, *104*, 334.
(30) Hediger, S.; Meier, B. H.; Ernst, R. R. *J. Chem. Phys.* **1995**, *102*, 4000.
(31) Jeffrey, G. A.; Saenger, W. *Hydrogen Bonding in Biological Structures*; Springer: Berlin/Heidelberg, 1991.
(32) Berglund, B.; Vaughan, R. W. *J. Chem. Phys.* **1980**, *73*, 2037.
(33) (a) Ditchfield, R. *J. Chem. Phys.* **1976**, *65*, 3123. (b) Rohlfing, C. M.; Allen, L. C.; Ditchfield, R. *J. Chem. Phys.* **1983**, *79*, 4958.
(34) Eckert, H.; Yesinowski, J. P.; Silver, L. A.; Stolper, E. M. *J. Phys. Chem.* **1988**, *92*, 2055.
(35) Yesinowski, J. P.; Eckert, H.; Rossman, G. R. *J. Am. Chem. Soc.* **1988**, *110*, 1367.
(36) Munowitz, M.; Pines, A. In *Advances in Chemical Physics*; 1987, *vol. LXVI*, p 1.
(37) Graf, R.; Demco, D. E.; Gottwald, J.; Hafner, S.; Spiess, H. W. *J. Chem. Phys.* **1997**, *106*, 885.
(38) Brown, S. P.; Spiess, H. W. *Chem. Rev.* **2001**, *101*, 4125.
(39) Hoatson, G. L.; Vold, R. L. In *NMR, Basic Principles and Progress*; Springer: Berlin, 1994, p 1.
(40) Fyfe, C. A.; Zhang, Y.; Aroca, P. *J. Am. Chem. Soc.* **1992**, *114*, 3252.
(41) Tekely, P.; Palmas, P.; Mutzenhardt, P. *Macromolecules* **1993**, *26*, 7363.
(42) Almond, G. G.; Harris, R. K.; Franklin, K. R. Solid State NMR **1996**, *6*, 31.
(43) Mehring, M. *Principles of High-Resolution NMR in Solids*; Springer: Berlin, 1983, p 151.
(44) Klur, I.; Jacquinot, J. F. Brunet, F.; Charpentier, T.; Virlet, J.; Schneider, C.; Tekely, P. *J. Phys. Chem. B* **2000**, *104*, 10 162.
(45) Vortmann, S.; Rius, J.; Siegmann, S.; Gies, H. *J. Phys. Chem. B* **1997**, *101*, 1292.
(46) Haeberlen, U. *Philos.Tran. R. Soc. London A* **1981**, *299*, 497.
(47) Butler, L. G.; Brown, T. L. *J. Am. Chem. Soc.* **1981**, *103*, 6541.
(48) Tekely, P.; Palmas, P.; Mutzenhardt, P. *J. Magn. Reson.* **1997**, *127*, 238.
(49) Di Beneditto, S.; Chidichimo, G.; Golemme, A.; Imbardelli, D. *J. Phys. Chem.* **1996**, *100*, 8079.
(50) Borowski, M.; Wolf, I.; Gies, H. *Chem. Mater.* **2002**, *14*, 38.